Biometals (2023) 36:549–562
https://doi.org/10.1007/s10534-022-00398-1

Deficiency of Lactoferrin aggravates lipopolysaccharide-induced acute inflammation via recruitment macrophage in mice

Can Liu · Qiu Peng · Lingyu Wei · Zhengshuo Li · Xiaoyue Zhang · Yangge Wu · Jia Wang · Xiang Zheng · Yuqing Wen · Run Zheng · Qun Yan · Qiurong Ye · Jian Ma

Received: 14 February 2022 / Accepted: 14 May 2022 / Published online: 1 June 2022

Abstract Lactoferrin (Lf), a multiple functional natural immune protein, is widely distributed in mammalian milk and glandular secretions (bile, saliva, tears and nasal mucosal secretions, etc.). In the previous study, we found that Lf plays an anti-inflammatory and anti-tumorigenesis role in AOM/DSS (azoxymethane/dextran sulfate sodium) induced mouse colitis-associated colon cancer model. Although we found that Lf has anti-inflammatory effects in chronic inflammation, its specific role and mechanisms in acute inflammation have not been clarified. Here, we reported that the expression levels of Lf were significantly increased when the organism was infected by Gram-negative bacteria. We then explored the role and potential mechanism of Lf in lipopolysaccharide (LPS)-induced acute inflammation. In the LPS-induced acute abdominal inflammation model, Lf deficiency aggravated inflammatory response and promoted macrophage chemotaxis to the inflammation site. Lf inhibited macrophage chemotaxis by suppressing the expression of macrophage-associated

Supplementary Information The online version contains supplementary material available at https://doi.org/10.1007/s10534-022-00398-1.

C. Liu · Q. Peng · J. Ma (✉)
Hunan Cancer Hospital and the Affiliated Cancer Hospital of Xiangya School of Medicine, Central South University, Changsha, China
e-mail: majian@csu.edu.cn

C. Liu · Q. Peng · Z. Li · X. Zhang · Y. Wu · Y. Wen · R. Zheng · J. Ma
Cancer Research Institute and School of Basic Medical Science, Central South University, Changsha, China

C. Liu · Q. Peng · Z. Li · X. Zhang · Y. Wu · Y. Wen · R. Zheng · J. Ma
Key Laboratory of Carcinogenesis and Cancer Invasion of the Chinese Ministry of Education, NHC Key Laboratory of Carcinogenesis, Hunan Key Laboratory of Nonresolving Inflammation and Cancer, Hunan Key Laboratory of Cancer Metabolism, Changsha, China

L. Wei
Department of Pathology, Heping Hospital Affiliated to Changzhi Medical College, Changzhi, Shanxi, China

J. Wang
Department of Immunology, Heping Hospital Affiliated to Changzhi Medical College, Changzhi, Shanxi, China

X. Zheng
Department of Pathology, Affiliated Hospital of Guilin Medical University, Guilin, Guangxi, China

Q. Yan
Department of Clinical Laboratory, Xiangya Hospital, Central South University, Changsha, China

Q. Ye (✉)
Department of Pathology, People's Hospital of Guangxi Zhuang Autonomous Region, Nanning, Guangxi, China
e-mail: yeqiurong1601@163.com

chemokines Ccl2 and Ccl5. Highly activated NF-κB signaling in $Lf^{-/-}$ mice was responsible for the high expression of Ccl2 and Ccl5. Our results suggested that the anti-inflammatory effect of Lf offers a new potential treatment for acute inflammatory diseases.

Keywords Lactoferrin · Chemokines · Acute inflammation

Introduction

Acute inflammation is an immediate series of processes of recognition, clearance and repair by the organism in response to pathogen invasion or self-damage (Varela et al. 2018). The main pathological changes in acute inflammation are involving in increased vascular permeability and leukocyte infiltration such as neutrophils, macrophages and lymphocytes (Ley et al. 2007; Wang and Kubes 2016). Lipopolysaccharide (LPS), a cell wall component of Gram-negative bacteria, is a major cause of acute inflammatory diseases such as sepsis, acute lung injury and acute liver injury (Domscheit et al. 2020; Joo et al. 2016; Rittirsch et al. 2007). In the LPS-induced acute inflammatory response, damaged tissues recruit macrophages by releasing large amounts of inflammatory factors and chemokines to promote the inflammatory response. Chemokines are peptides or proteins with molecular sizes of about 8–12 kDa and are involved in the activation of immune cells and chemotaxis of lymphocytes (Luster 1998). In acute inflammation, CCL2 and CCL5 play an important role in the chemotaxis of monocytes-macrophages toward the inflammatory sites (Dal-Secco et al. 2015). The timely recruitment and regression of inflammatory macrophages play an important role in the maintenance of homeostasis after acute inflammation (Vannella and Wynn 2017).

Lactoferrin (Lf) is a multifunctional natural immune iron-binding glycoprotein with a molecular size of about 80 kDa, and is widely distributed in mammalian milk and glandular secretions (bile, saliva, tears, and nasal mucosal secretions, etc.). Due to its broad-spectrum anti-bacterial, anti-viral and anti-cancer ability and iron-binding capability, Lf has been widely used in infant formula (Wang et al. 2019), nutraceuticals (Superti 2020), and nanoparticle-based delivery systems (Elzoghby et al. 2020) with a promising prospect. In our previous study, we established *Lf* knockout ($Lf^{-/-}$) mice, and found that Lf exerts anti-inflammatory and anti-cancer effects in the AOM/DSS (azoxymethane/dextran sulfate sodium)-induced ulcerative colitis-carcinoma mouse model (Ye et al. 2014). The anti-inflammatory and antibacterial effects of Lf have been reported in several previous studies (Cutone et al. 2019; Velusamy et al. 2013; Wu et al. 2016), and the potential mechanism of its anti-inflammatory effect is mediated by down-regulating the expression levels of pro-inflammation cytokines (such as IL-1β, IL-6, and TNF-α) and up-regulating the expression levels of anti-inflammation cytokines (such as IL-4 and IL-10), while the more detailed mechanism needs to be studied.

Although we found that Lf has an anti-inflammatory effect in DSS-induced chronic inflammation, its role and potential mechanism in acute inflammation have not been clarified. In the present study, we revealed that Lf plays an important anti-inflammatory role in LPS-induced acute inflammation. Lf exerts its anti-inflammation role by suppressing the chemotaxis of macrophages towards the inflammation sites. This finding provides a potential new strategy for the treatment of acute inflammatory diseases.

Materials and methods

Mice and cell line

The *Lf* knockout ($Lf^{-/-}$) mice were generated on C57B/L6 background as reported previously (Ye et al. 2014). Mouse macrophage cell Raw264.7 was grown in RPMI-1640 with 10% fetal bovine serum and Penicillin–Streptomycin. Generation of mouse embryonic fibroblasts (MEF) from WT or $Lf^{-/-}$ mice was followed by the protocol (Xu 2005). MEF was grown in DMEM medium with 10% fetal bovine serum and Penicillin–Streptomycin. This study was approved by the Animal Ethics Committee of Central South University (China), and animal experiments in the current study were carried out in strict accordance with the approved research protocol.

LPS-induced acute inflammation in mice and MEF cell

The littermate male WT and $Lf^{-/-}$ mice (6–8 weeks) were weighed and injected intraperitoneally with LPS (L9143, Sigma–Aldrich) at a dose of 4 mg/kg to induce acute inflammation response (or with an equal volume of PBS as the control group, each group n = 5). For Cenicriviroc treatment experiment, the mice were intraperitoneally injected with Cenicriviroc (CVC, 10 mg/kg, Selleck) 10 min prior to LPS injection. 4 h later, the mice were weighed again (each group n = 3). Serum was collected and stored at − 80 °C. The mice were injected intraperitoneally with 5 ml of RPMI-1640 after euthanasia, and the peritoneal lavage fluid was collected and centrifuged to obtain the lavage fluid supernatant and peritoneal cells. The WT and $Lf^{-/-}$ MEF cells were stimulated by LPS (1 μg/ml) or PBS for 4 h, and BAY11-7082 (1 μM, APExBIO) is added to inhibit the NF-κB pathway.

Histological analysis and immunohistochemistry

Mouse liver tissue was fixed in fresh 4% paraformaldehyde for 24 h. After dehydration and paraffin embedding, 4 μm thick paraffin sections were obtained. The level of acute inflammatory response is assessed by the percentage of total tissue area infiltrated by inflammatory cells, and sections with a high percentage of infiltration are thought to carry a stronger level of inflammatory response. The measurement of the area infiltrated by inflammatory cells and total tissue area is completed by ImageJ software. For the immunohistochemistry analysis, after antigen-retrieval, liver tissue paraffin sections were blocked with 5% goat serum to reduce non-specific binding, then incubated with primary antibody overnight at 4 °C, p65 (1:500, Cell Signaling Technology), Lf (1:500, servicebio), MPO (1:500, R&D). Then, the sections were incubated with the HRP-conjugated secondary antibodies (ZSGB-Bio) for 1 h at 37 ℃, and the staining was visualized by diaminobezidin-3 (DAB, ZSGB-Bio).

Western blot

The protein was extracted by RIPA lysate buffer (Beyotime) with protease inhibitor cocktail and phosphatase inhibitor cocktail (Bimake). After separation by SDS-page gel, the protein was transferred to the PVDF membrane (Millipore) and blocked with 5% skim milk. Then, the primary antibody was incubated overnight at 4 ℃, p65 (1:1000, Cell Signaling Technology), p65 ser536 (1:1000, Cell Signaling Technology), and the corresponding secondary antibody was incubated at 37℃. Blot images were detected by an enhanced chemiluminescence kit (Millipore).

Enzyme linked immunosorbent assay (ELISA)

The serum and peritoneal lavage fluid were harvested from LPS-injected or PBS-injected mice. The concentration of inflammatory cytokines tumor necrosis factor-α (TNF-α), interleukin-6 (IL-6) interleukin-1β (IL-1β) in serum and peritoneal lavage fluid was measured by the commercial ELISA kits according to the manufacturer's protocols (Boster, China).

RNA-sequencing and bioinformatics analysis

The peritoneal cells were collected from the LPS- or PBS-injected mice. The control group mice (either WT or $Lf^{-/-}$) were injected with PBS. The LPS group mice (either WT or $Lf^{-/-}$) were injected with LPS (4 mg/kg). Three independent biological replicates per subgroup (12 samples in total) were extracted following the manufacturer's protocol (Oebiotech, Shanghai, China). After RNA integrity was evaluated, libraries were constructed and sequenced on the Illumina sequencing platform (HiSeq 2500). The RNA-seq raw expression files and details have been deposited in NCBI GEO under accession number GSE181752. The differently expressed genes between WT and $Lf^{-/-}$ group were selected with a threshold of $p < 0.05$ and fold change > 1.2 or < 0.8. The upregulated genes in $Lf^{-/-}$ group were analyzed with GO enrichment analysis and KEGG pathway analysis by DAVID Bioinformatics Resources 6.8 (https://david.ncifcrf.gov/). Gene Set Enrichment Analysis (GSEA, https://www.gsea-msigdb.org/gsea/index.jsp) was used to compare the difference in gene expression landscape between WT and $Lf^{-/-}$ group after LPS stimulation. Publicly available datasets (GSE6269, GSE69528, GSE46356, and GSE4764) were downloaded from the gene expression omnibus (GEO, https://www.ncbi.nlm.nih.gov/geo/).

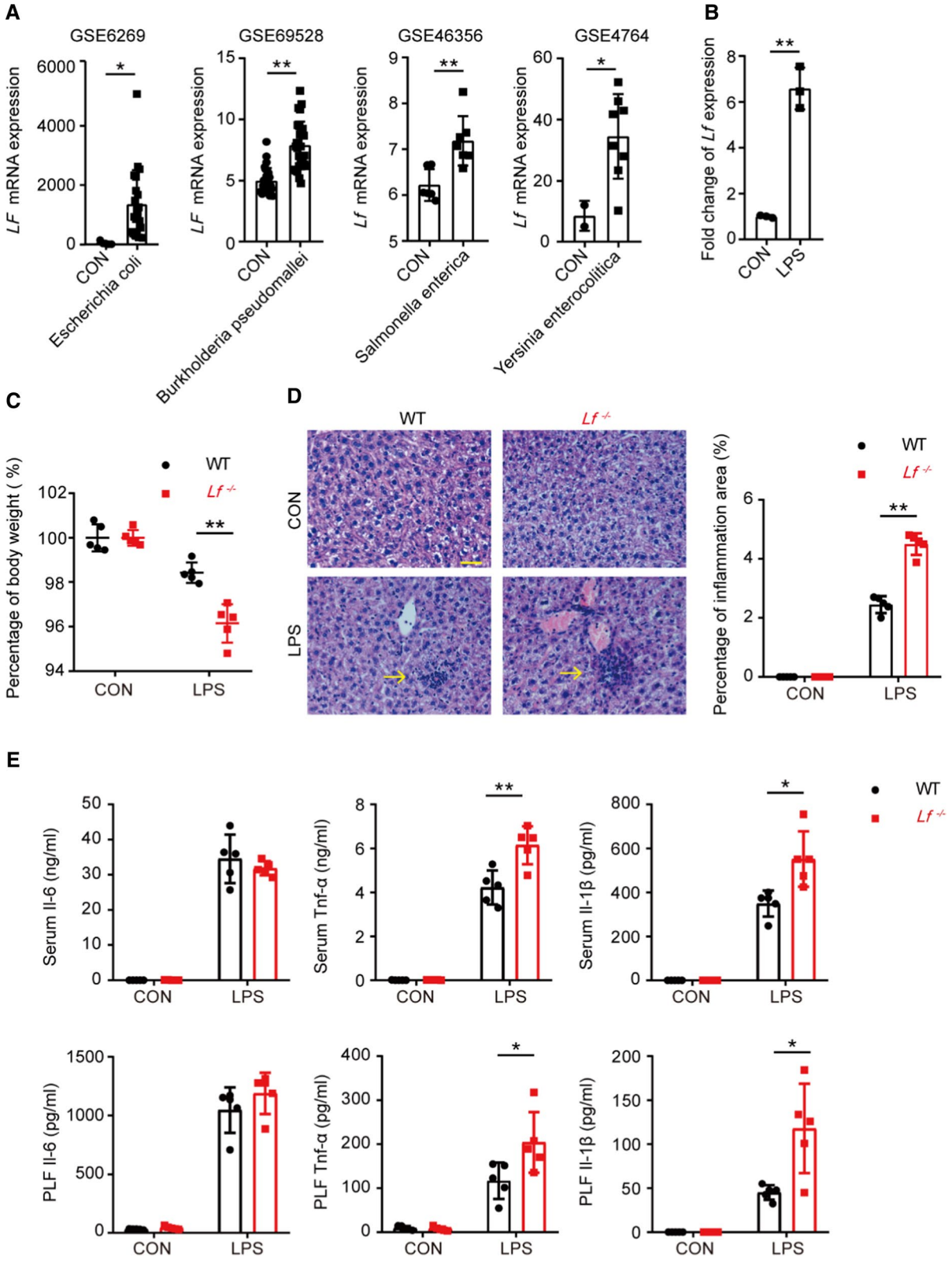
A
GSE6269
GSE69528
GSE46356
GSE4764
LF mRNA expression
Lf mRNA expression
CON
Escherichia coli
Burkholderia pseudomallei
Salmonella enterica
Yersinia enterocolitica
B
Fold change of Lf expression
CON
LPS
C
Percentage of body weight (%)
WT
Lf -/-
CON
LPS
D
WT
Lf -/-
CON
LPS
Percentage of inflammation area (%)
E
Serum Il-6 (ng/ml)
Serum Tnf-α (ng/ml)
Serum Il-1β (pg/ml)
PLF Il-6 (pg/ml)
PLF Tnf-α (pg/ml)
PLF Il-1β (pg/ml)

◂**Fig. 1** Lactoferrin deficiency in mice aggravates LPS-induced acute inflammation. **A** *LF* gene expression levels in the uninfected and Gram-negative bacterial infected group (dataset from GSE6269, GSE69528, GSE46356, and GSE4764). **B** The littermate Male WT and $Lf^{-/-}$ mice were injected intraperitoneally with LPS at a dose of 4 mg/kg (or with an equal volume of PBS as the CON group) to induce an acute inflammation response. *Lf* gene expression levels in the unstimulated and LPS stimulated group in mice peritoneal cells(n = 3). **C** The body weight change of WT and $Lf^{-/-}$ mice after PBS or LPS injection (n = 5). **D** The histological analysis of the liver tissues from WT and $Lf^{-/-}$ mice after PBS (CON) or LPS injection (n = 5). The yellow arrow indicated the inflammation site and the bar indicated 50 μm. (E) The concentration of Il-6, Tnf-α, and Il-1β in the serum and peritoneal lavage fluid from WT and $Lf^{-/-}$ mice after PBS or LPS injection (n = 5). The student's t-test was used to compare two groups; the one-way ANOVA test was used to compare multiple groups. *$p < 0.05$, **$p < 0.01$. (Color figure online)

Flow cytometry

Single-cell suspensions from peritoneal lavage fluid were filtered by cell strainer (70 μm), followed by red blood cell lysis. Then, 1×10^6 cells were added into tubes and washed with cold PBS. And cells were incubated with mixed combinations of antibodies for 30 min at 4 °C. Information on the antibodies (BioLegend, CA, USA) used is as follows: APC-F4/80 (1:100), FITC-CD11b (1:100), PE/DAZZLE 594-CD45 (1:100), Zombie Aqua™ Fixable Viability Kit (1:500). The data were detected by DxpAthena (Cytek, USA) and analyzed by FlowJo software (TreeStar Olten, Switzerland).

Immunofluorescence

After antigen-retrieval, liver tissue paraffin sections were blocked with 5% goat serum to reduce nonspecific binding, then incubated with CD68 (1:200, Proteintech, China) primary antibody overnight at 4 °C. Then, the sections were incubated with the Cy3-conjugated secondary antibodies (1:500, Proteintech, China). The nuclei were labeled with 4′,6-diamidino-2-phenylindole (DAPI, Bioss, China). Images were obtained with a fluorescence microscope.

Quantitative real-time PCR

Total RNA was isolated from peritoneal cells using RNeasy Kits (Qiagen, Germany) according to the manufacturer's instructions, followed to synthesize cDNA by means of a Revert Aid First Strand cDNA Synthesis Kit (Thermo Fisher, USA). The primers sequence is as follows: *Tnf-α*: forward 5′-AGC GGATGGGTTGTACCTTG-3′, reverse 5′-GTG GGTGAGGAGCACGTAGTC-3′; *Il-1β*: forward 5′-TTTTCCTCCTTGCCTCTGAT -3′, reverse 5′-GAGTGCTGCCTAATGTCCCC-3′; *Ccl2*: forward 5′-TTAAAAACCTGGATCGGAACCAA -3′, reverse 5′-GCATTAGCTTCAGATTTACGGGT-3′; *Ccl5*: forward 5′-GCTGCTTTGCCTACCTCT CC-3′, reverse 5′-TCGAGTGACAAACACGAC TGC-3′; *Gapdh:* forward 5′-CAGCCCCGGCAT CGAAGGTG-3′, reverse 5′-TCTGACGTGCCG CCTGGAGA-3′. The relative target gene mRNA levels were quantified by measuring cycle threshold (Ct) values and normalized to *Gapdh*.

Macrophage chemotaxis assay

The supernatants of peritoneal lavage fluid were diluted 10 folds with RPMI-1640 medium and then added to the lower chamber of the transwell plate (3422, Costar), 1×10^4 mouse macrophage Raw246.7 cells in 100 μl were added into the upper chamber (8 μm), incubated for 36 h at 37 °C. Fixed the upper chamber in 4% paraformaldehyde for 20 min, washed twice, and stained with 0.1% crystal violet staining solution (Bioss, China) for 20 min. The cells in the upper chamber layer were wiped away and the migrated cells were observed with a light microscope.

Statistical analysis

Statistical software SPSS 22.0, GraphPad Prism 5, and R 4.0.2 were used to analyze the data in this

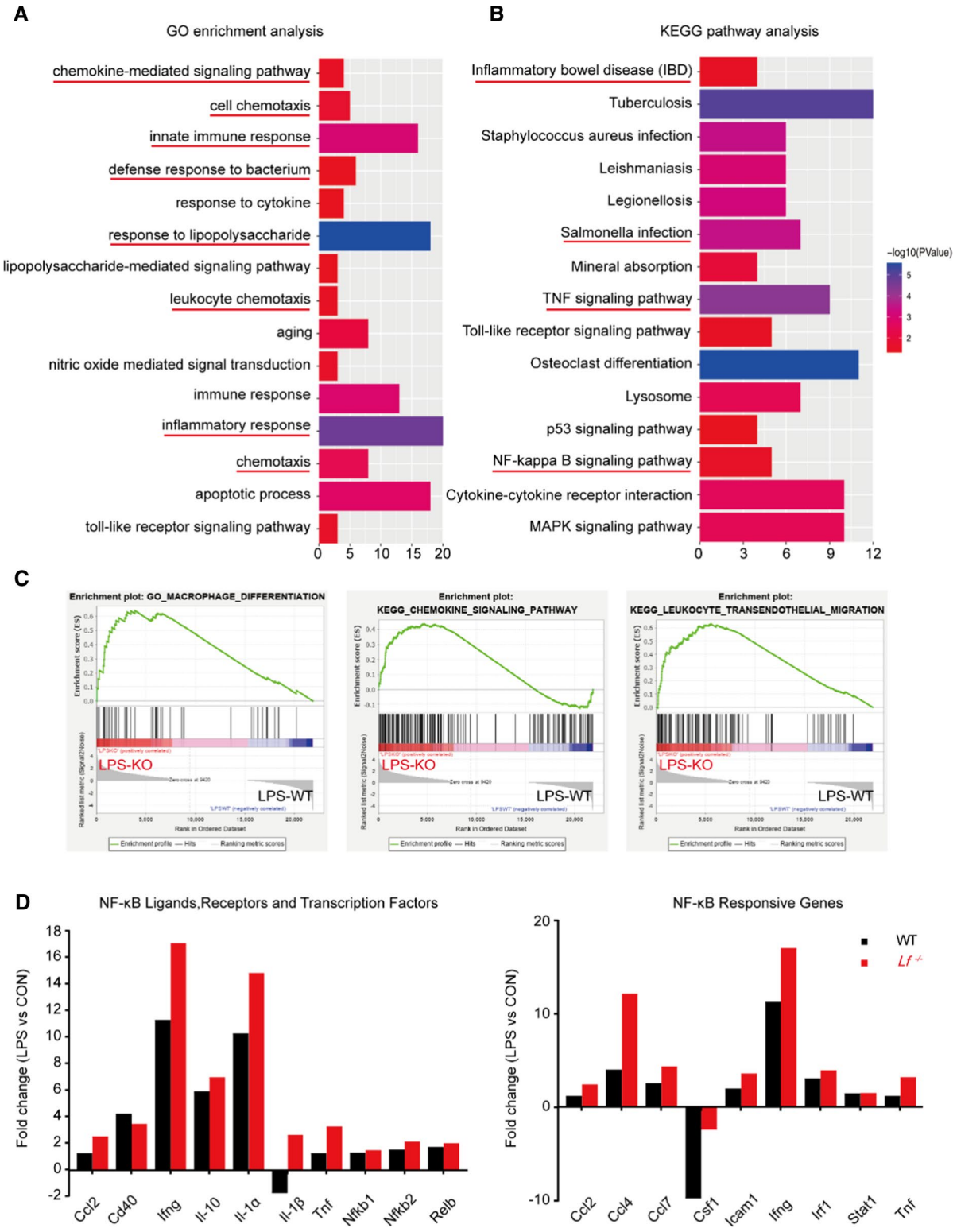
A
GO enrichment analysis
chemokine-mediated signaling pathway
cell chemotaxis
innate immune response
defense response to bacterium
response to cytokine
response to lipopolysaccharide
lipopolysaccharide-mediated signaling pathway
leukocyte chemotaxis
aging
nitric oxide mediated signal transduction
immune response
inflammatory response
chemotaxis
apoptotic process
toll-like receptor signaling pathway
0 5 10 15 20
B
KEGG pathway analysis
Inflammatory bowel disease (IBD)
Tuberculosis
Staphylococcus aureus infection
Leishmaniasis
Legionellosis
Salmonella infection
Mineral absorption
TNF signaling pathway
Toll-like receptor signaling pathway
Osteoclast differentiation
Lysosome
p53 signaling pathway
NF-kappa B signaling pathway
Cytokine-cytokine receptor interaction
MAPK signaling pathway
0 3 6 9 12
-log10(PValue)
5
4
3
2
C
Enrichment plot: GO_MACROPHAGE_DIFFERENTIATION
Enrichment plot: KEGG_CHEMOKINE_SIGNALING_PATHWAY
Enrichment plot: KEGG_LEUKOCYTE_TRANSENDOTHELIAL_MIGRATION
LPS-KO
LPS-WT
Rank in Ordered Dataset
Enrichment profile
Hits
Ranking metric scores
D
NF-κB Ligands,Receptors and Transcription Factors
Fold change (LPS vs CON)
Ccl2
Cd40
Ifng
Il-10
Il-1α
Il-1β
Tnf
Nfkb1
Nfkb2
Relb
NF-κB Responsive Genes
WT
Lf -/-
Ccl2
Ccl4
Ccl7
Csf1
Icam1
Ifng
Irf1
Stat1
Tnf

◂**Fig. 2** Lactoferrin deficiency alters gene's inflammatory signalings. **A**, **B** GO analysis and KEGG analysis of differential genes up-regulated in the $Lf^{-/-}$ mice (vs WT) after LPS stimulation. **C** GSEA analysis between WT and $Lf^{-/-}$ mice after LPS stimulation. **D** Fold change of NF-κB pathway genes expression levels between WT and $Lf^{-/-}$ mice after LPS stimulation (LPS vs CON). (Color figure online)

study. The student's t-test was used to compare two groups; the one-way ANOVA test was used to compare multiple groups. The differences were considered statistically significant if $p < 0.05$, and $p < 0.05$ indicated by "*", $p < 0.01$ is indicated by "**", $p < 0.001$ is indicated by "***".

Results

Lf deficiency in mice aggravates LPS-induced acute inflammation

Bacterial infection is the main cause of acute inflammation. Through analyzing the NCBI GEO database, we noticed that the expression levels of Lf were significantly increased when the organism was infected by gram-negative bacteria (Fig. 1A), such as *Escherichia coli* (GSE6269) (Xiao et al. 2021), *Burkholderia pseudomallei* (GSE69528) (Khaenam et al. 2014), *Salmonella enterica* (GSE46356) (Bellet et al. 2013) and *Yersinia enterocolitica* (GSE4764) (Handley et al. 2006), which suggests that Lf may play a particular role in acute inflammation caused by gram-negative bacteria infections. To investigate the relationship between Lf and acute inflammation, we utilized LPS to establish an acute inflammation model in $Lf^{-/-}$ mice to mimic the process of bacterial infection. LPS (or PBS as negative control) was injected intraperitoneally into wild-type (WT) and $Lf^{-/-}$ mice to induce acute inflammation in the abdominal cavity. We found that Lf expression levels in peritoneal cells were significantly elevated after LPS was injected into mice compared to that in PBS injection (Fig. 1B). $Lf^{-/-}$ mice lost more weight than WT mice in LPS-induced acute inflammation (Fig. 1C). To investigate the pathological changes in mouse liver tissue after LPS stimulation, H&E staining was performed on the liver tissue sections. In the PBS-injected group, no inflammatory cells or features were observed in the liver tissue of both WT and $Lf^{-/-}$ mice, whereas in the LPS-injected group, the liver tissue of WT and $Lf^{-/-}$ mice showed varying degrees of inflammatory cells infiltration, and the $Lf^{-/-}$ mice had higher levels of inflammatory cells infiltration (Fig. 1D), and in liver tissue, Lf expression is increased after LPS injected which may be attributed to the increase of neutrophils in liver tissue after LPS stimulation (Fig. S1). We collected mice peritoneal lavage fluid and serum, and measured the concentration of inflammatory factors such as Il-6, Tnf-α and Il-1β by ELISA. The concentration of Tnf-α and Il-1β of $Lf^{-/-}$ mice were significantly higher than that of WT mice in the LPS-induced acute inflammation model (Fig. 1E). These results suggest that Lf deficiency aggravates LPS-induced acute inflammation.

Lf deficiency alters gene's inflammatory signalings

To further investigate the potential mechanisms of how the Lf deficiency aggravates LPS-induced acute inflammation, mRNA sequencing was utilized to depict the alteration of gene expression profiles of peritoneal cells upon LPS stimulation. In the peritoneal cells, there were 167 genes upregulated and 45 genes were downregulated in $Lf^{-/-}$ mice compared with that in WT mice. The detailed genes were listed in Supplementary Table 1. The 167 upregulated genes ($Lf^{-/-}$ vs WT) were analyzed with GO and KEGG analysis. The GO enrichment analysis revealed that the process of the inflammatory response, response to lipopolysaccharide, response to molecule of bacterial origin, and innate immune response were enriched, which means inflammatory response in $Lf^{-/-}$ mice was more severe than that in WT mice. Besides, the process of chemotaxis was more activated in $Lf^{-/-}$ mice (Fig. 2A). The KEGG pathway analysis revealed that the process of inflammatory bowel disease (IBD), Salmonella infection, and NF-κB signaling pathway were enriched in $Lf^{-/-}$ mice (Fig. 2B). Gene Set Enrichment Analysis (GSEA) revealed that processes of macrophage differentiation, chemokine signaling, and leukocyte transendothelial migration were enriched in $Lf^{-/-}$ group (Fig. 2C). We next compared the gene expression changes of NF-κB pathway between WT and $Lf^{-/-}$ group in the peritoneal cells after stimulation with LPS (LPS vs CON). The fold change of NF-κB responsive genes Ccl2, Ccl4, Ccl7, Il-1β, Ifng, Il-1α, Tnf, and Nfkb2 were higher in the $Lf^{-/-}$ group (Fig. 2D). This suggested that in LPS-induced acute inflammation, Lf deficiency may cause increased activation of the NF-κB signaling pathway,

promoting increased secretion of chemokines and inflammatory factors.

Lf$^{-/-}$ mice recruit more macrophages in LPS-induced acute inflammation

Macrophages play a curial role in the acute inflammation process (Na et al. 2019). As hinted by the mRNA sequencing analysis (Fig. 2), we compared the proportion of peritoneal macrophages between WT and *Lf*$^{-/-}$ mice by flow cytometry. The proportion of peritoneal macrophages in the *Lf*$^{-/-}$ mice was significantly higher than in the WT mice upon LPS stimulation (Figs. 3A, B), while no difference was observed in the CON group (i.e. PBS injection). Meanwhile, we tested the mRNA expression levels of

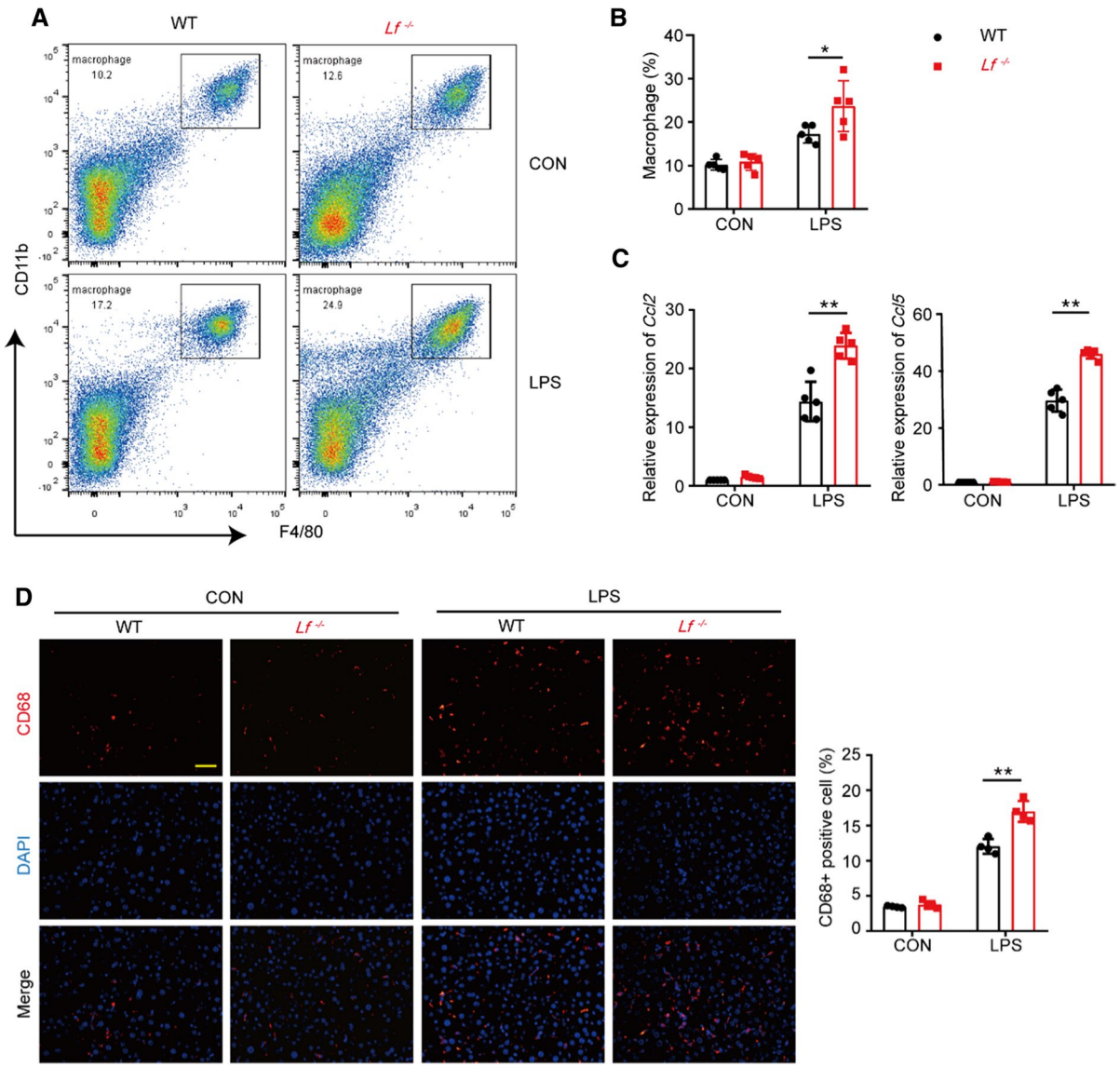

Fig. 3 *Lf*$^{-/-}$ mice recruit more macrophages in LPS-induced acute inflammation. **A**, **B** The percentage of mice peritoneal macrophages in WT and *Lf*$^{-/-}$ mice after PBS (CON) or LPS injection (n = 5). **C** The relative mRNA expression levels of *Ccl2* and *Ccl5* (n = 5) in mice peritoneal macrophages from WT and *Lf*$^{-/-}$ mice after LPS injection (based on PBS injected WT mice). **D** The distribution of macrophages ($CD68^{+}$) in mouse liver tissue from WT and *Lf*$^{-/-}$ mice after PBS or LPS injection. The bar indicated 50 μm, and $^{*}p < 0.05$, $^{**}p < 0.01$. (Color figure online)

macrophage-related chemokines Ccl2 and Ccl5 (two of the most important chemokines for macrophages) in the peritoneal cells, and found that the mRNA expression levels of Ccl2 and Ccl5 were significantly higher in $Lf^{-/-}$ mice than that in WT group after LPS injection (Fig. 3C). Then, we investigated the distribution of macrophages ($CD68^{+}$) in mouse liver tissue by immunofluorescence experiments. A higher proportion of macrophages in the liver tissue section was observed in $Lf^{-/-}$ mice compared to WT mice under the LPS stimulation (Fig. 3D). Those results revealed that under the circumstances of LPS-induced acute inflammation, $Lf^{-/-}$ mice have higher levels of macrophage chemokines, and could recruit more macrophages at the inflammation site.

Lf suppresses macrophage chemotaxis and alleviates inflammatory response

Ccl2 and Ccl5 are macrophage chemokines, and their elevated concentrations in local tissues attract macrophages from the circulation. Cenicriviroc (CVC), an experimental candidate for the treatment of HIV infection, is a co-inhibitor of the Ccr2/Ccr5 (Ccl2/Ccl5 receptor). We asked whether $Lf^{-/-}$ mice recruiting more macrophages was due to (or partially due to) the elevation of the two chemokines, Ccl2 and Ccl5. An in vitro macrophage chemotaxis assay was employed here. The supernatants of peritoneal lavage fluid from PBS-injected or LPS-injected mice were 1:10 diluted, then added in the lower chamber of the transwell to assess their effects on the chemotactic ability of mouse macrophage Raw246.7 cells which in the upper chamber. The experimental groups were divided by the source of the peritoneal lavage fluid and treatment: the control group used peritoneal lavage fluid from PBS-injected mice (WT or $Lf^{-/-}$); the LPS group used peritoneal lavage fluid from LPS-injected mice (WT or $Lf^{-/-}$); the LPS + CVC group used peritoneal lavage fluid from LPS-injected mice (WT or $Lf^{-/-}$) and then was treated with CVC (final concentration 1 μM). The number of Raw246.7 cells migrating to the lower chamber was significantly higher in the LPS-$Lf^{-/-}$ group than that in the LPS-WT group, and CVC partially inhibited the chemotaxis of Raw246.7 cells (Fig. 4A). We next examined the effect of CVC in vivo. The three groups are CON (control), LPS, and LPS + CVC group, and mice in CON group were injected with PBS, mice in LPS group were injected with LPS, mice in LPS + CVC group were injected with LPS and CVC. The distribution of macrophages ($CD68^{+}$) in liver tissue was detected by immunofluorescence. The proportion of macrophages in the liver tissues of LPS group was higher than that of CON group, and the Ccr2/Ccr5 inhibitor CVC was effective in reducing the proportion of macrophages in the livers of LPS-stimulated mice, and the proportion of macrophages in the liver of $Lf^{-/-}$ mice was higher than that in WT mice after LPS stimulation (Figs. 4B, C). The mRNA expression levels of inflammatory factors Tnf-α and Il-1β in the peritoneal cells of $Lf^{-/-}$ mice were significantly higher than that in WT mice after LPS injection, and CVC reduced their expression levels (Fig. 4D). In addition, CVC effectively alleviated the inflammatory response in the liver tissues induced by LPS stimulation (Fig. 4E). These results indicated that Lf exerts an anti-inflammatory effect by suppressing the expression levels of macrophage-associated chemokines Ccl2 and Ccl5, thus inhibiting macrophage chemotaxis in a mouse model of LPS-induced acute inflammation.

Lf alleviates macrophage chemotaxis via suppressing the activation of the NF-κB signaling pathway

Immunohistochemistry assay revealed that the NF-κB p65 expression levels in liver tissues of $Lf^{-/-}$ mice were higher than that of WT mice after LPS stimulation (Fig. 5A). When the LPS was given to WT and $Lf^{-/-}$ mouse embryonic fibroblasts (MEF), we found that the expression levels of P65 and phosphorylation levels of p65 ser536 in $Lf^{-/-}$ MEF were significantly higher than those in WT MEF after LPS stimulation. While, after giving 1 μM NF-κB inhibitor BAY11-7082, highly activated p65 was effectively attenuated in $Lf^{-/-}$ MEF (Fig. 5B). In addition, inhibition of the activating p65 suppressed the expression levels of Ccl2 and Ccl5 (Fig. 5C). Those results revealed that Lf deficiency induced highly activated p65 is responsible for macrophage aggregation in the acute inflammation response.

Discussion

In this study, we utilized $Lf^{-/-}$ mice to investigate the role of Lf in LPS-induced acute inflammation.

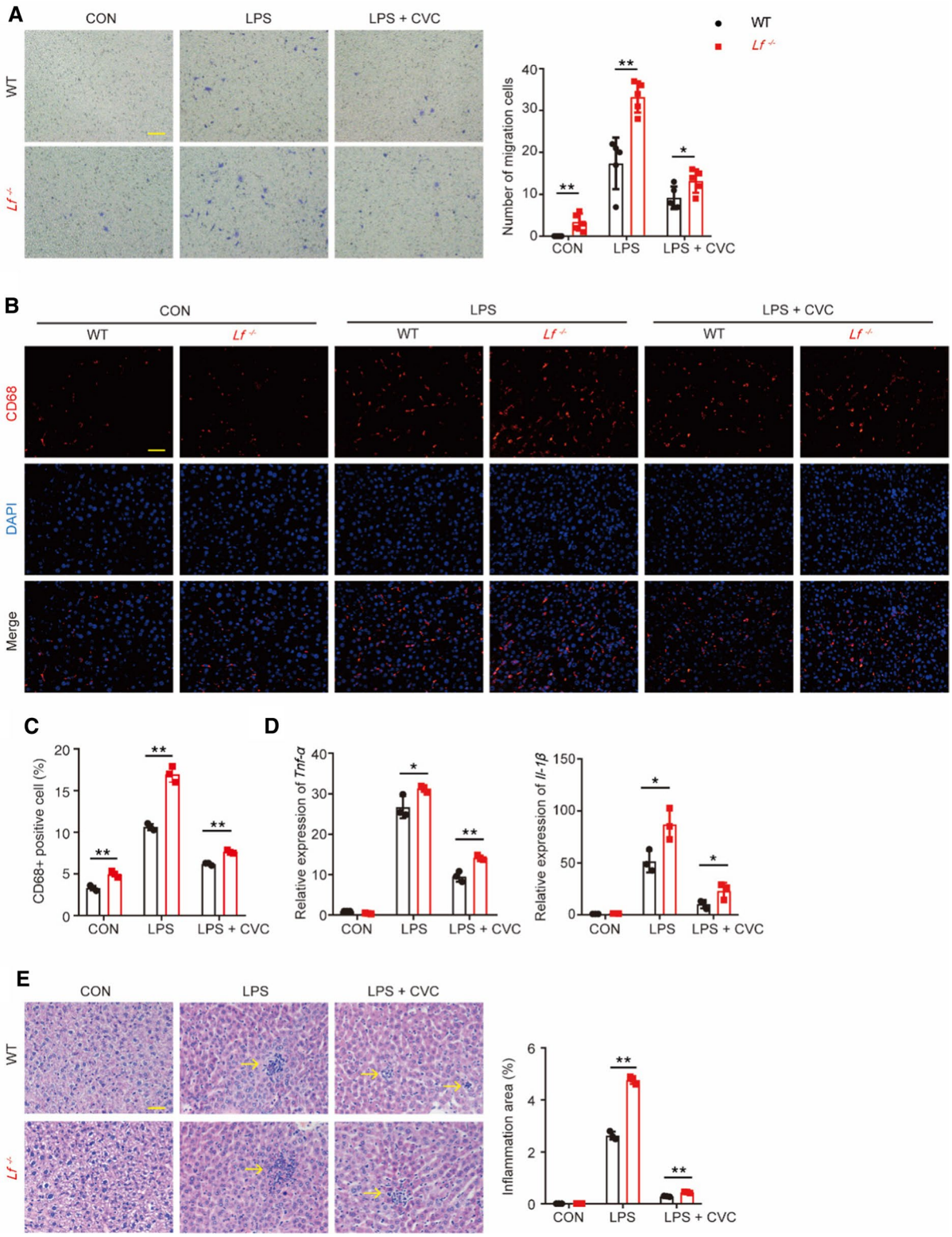
A
CON
LPS
LPS + CVC
WT
Lf -/-
Number of migration cells
B
CD68
DAPI
Merge
C
CD68+ positive cell (%)
D
Relative expression of Tnf-α
Relative expression of Il-1β
E
Inflammation area (%)

◂**Fig. 4** Lactoferrin suppresses macrophage chemotaxis and alleviates inflammatory response. **A** The macrophage chemotaxis ability of peritoneal lavage fluid from WT and $Lf^{-/-}$ mice after PBS or LPS injection (n = 5) was assessed by transwell migration assay, and the bar indicated 100 μm. **B**, **C** The distribution of macrophages ($CD68^{+}$) in mouse liver tissue from WT and $Lf^{-/-}$ mice after PBS, LPS or CVC treatment (n = 3), and the bar indicated 50 μm. **D** The relative mRNA expression levels of *Tnf-α* and *Il-1β* (n = 3) in mice peritoneal macrophages from WT and $Lf^{-/-}$ mice after LPS injection (based on PBS injected WT mice). **E** The histological analysis of the liver tissues from WT and $Lf^{-/-}$ mice after PBS, LPS or CVC treatment (n = 3), and the bar indicated 50 μm. *p < 0.05, **p < 0.01. (Color figure online)

Our results show that deficiency of Lf aggravates the acute inflammatory response; and $Lf^{-/-}$ mice show stronger chemotaxis of macrophages to the inflammation site than WT mice through an increase in the expression of chemokines Ccl2 and Ccl5. Inhibition of macrophage chemotaxis effectively reduced the levels of inflammation response. Besides, highly activated p65 signaling in $Lf^{-/-}$ mice is responsible for the high expression of Ccl2 and Ccl5 (Fig. 6).

Lf, secreted by exocrine glands and by neutrophils, is an iron-binding multifunctional cationic glycoprotein, and it usually functions as iron ion transport together with transferrin, which might be the possible mechanisms for inhibiting bacterial proliferation and inhibit inflammation. Aerosolized bovine Lf was reducing pulmonary bacterial load, pulmonary iron overload, and infiltrating leukocytes in a cystic fibrosis mouse model of *Pseudomonas aeruginosa* chronic lung infection (Cutone et al. 2019). On the other hand, Lf exerted its anti-inflammation role by direct binding with the LPS of Gram-negative bacteria (Brandenburg, et al. 2001). Lf may prevent injury-induced oxidative stress and subsequent 'cytokine storm', hence, it has the potential to reduce SARS-CoV-2-induced cytokine storm (Zimecki, et al. 2021), and was proposed for a clinical trial to evaluate and verify its effect in COVID-19 pandemic (Campione et al. 2020). During clinical trials, enteral Lf supplementation decreased sepsis and necrotizing enterocolitis in preterm infants (Pammi et al. 2017). Although several studies have previously reported that Lf reduces inflammation induced by gram-negative

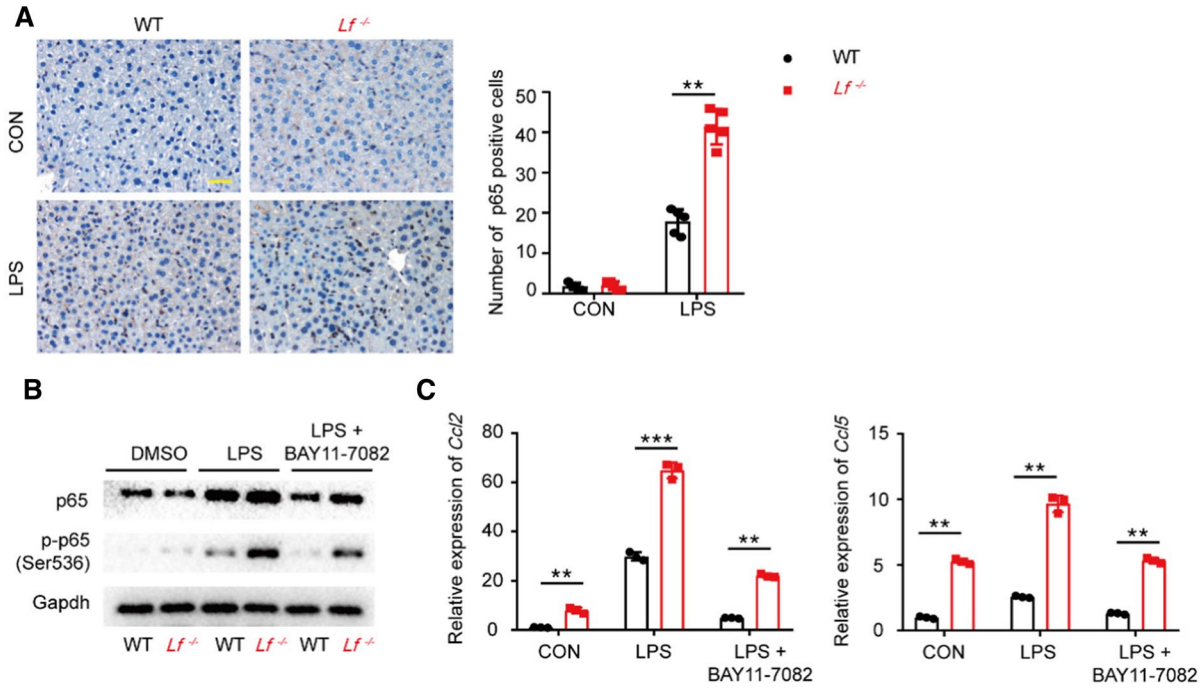

Fig. 5 Lactoferrin suppresses the activation of NF-κB p65. **A** The NF-κB p65 expression levels in mouse liver tissue from WT and $Lf^{-/-}$ mice after PBS or LPS injection. **B** Cell lysates were analyzed by Western blotting to detect the expression of p65 and phosphorylation levels of p65 ser536 in MEF from WT and $Lf^{-/-}$ mice after LPS or BAY11-7082 treatment. **C** The relative mRNA expression levels of *Ccl2* and *Ccl5* (n = 3) in MEF from WT and $Lf^{-/-}$ mice after LPS or BAY11-7082 treatment. The bar indicated 50 μm, and *p < 0.05, **p < 0.01 and ***p < 0.001. (Color figure online)

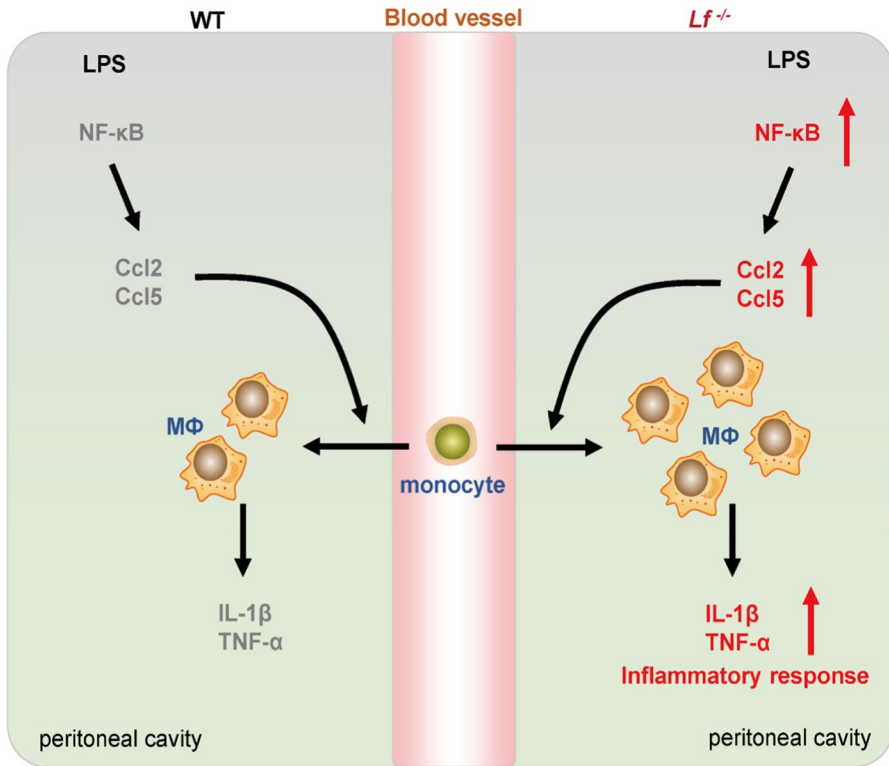

Fig. 6 A schematic diagram demonstrating that lactoferrin suppresses the LPS-induced inflammation via alleviating the chemotaxis of macrophages. (Color figure online)

bacterial infections such as *Pseudomonas aeruginosa* (Cutone et al. 2019), *Salmonella enterica serovar typhimurium* (Wu et al. 2016) and *Aggregatibacter actinomycetemcomitans* (Velusamy et al. 2013), the detailed mechanism has not been elucidated.

In an in vitro experiment, resolution-associated Lf peptides limited inflammation by inhibiting the expression of inflammatory factors in macrophages (Lutaty A et al. 2020). In the present study, we found that Lf exerted an anti-inflammatory effect by inhibiting the chemotaxis of macrophages towards the inflammatory sites, and the activation of the NF-κB pathway, the most important inflammatory signaling, was significantly higher in $Lf^{-/-}$ mice after LPS stimulation comparing to WT mice. Gene expression profiling suggested that Lf may inhibit the expression of chemokines Ccl2 and Ccl5 by suppressing the activation of the NF-κB pathway, thereby inhibiting the chemotaxis of macrophages towards inflammatory sites. It is not a surprise that Lf could inhibit macrophage chemotaxis in the acute inflammation response, for the immunomodulatory function of Lf has been revealed in previous studies: Liu et al. reported that lactoferrin-induced myeloid-derived suppressor cells (MDSC) were effective in blocking inflammation in the newborn mice with necrotizing enterocolitis, and increasing survival (Liu et al. 2019). We reported that Lf deficiency facilitated mouse melanoma cells B16 metastasizing to the lungs, through modulating the immune microenvironment in the lungs (Wei et al. 2020). We also reported that Lf is an important factor in regulating early B-cell development (Wei et al. 2021).

Acute inflammation response is an important protective mechanism employed by our body against infection, injury, etc. Removing pathogens and repairing damaged tissue both require an inflammatory response; however, an uncontrolled inflammatory response can cause damage to the host. The molecular mechanisms that negatively regulate inflammatory signaling are only beginning to be understood. Here, we found that Lf is significantly upregulated in the inflammation response, and deficiency of Lf could aggravate LPS-induced acute inflammation. We revealed a possible relationship between Lf, macrophage chemotaxis and acute inflammation, and

identified that Lf is an anti-inflammation molecule through modulating chemokines and macrophage chemotaxis. The current study suggests that Lf is a potential new medicine nutrient for the treatment of acute inflammatory diseases.

Conclusions

We revealed that Lf exerts its anti-inflammation role in LPS-induced acute inflammation by suppressing the expression levels of macrophage-associated chemokines Ccl2 and Ccl5, and highly activated p65 signaling in $Lf^{-/-}$ mice is responsible for the high expression of Ccl2 and Ccl5. Hence, Lf suppresses the chemotaxis of macrophages towards the inflammation tissue to alleviate acute inflammation response through inhibiting NF-κB signaling.

Acknowledgements This work was supported by the National Natural Science Foundation of China (81660273, 81672889, 82101907, 82060042, 32000665), China 111 Project (111-2-12), Natural Science Foundation of Changsha (kq2014297, kq2202125), Hunan Natural Sciences Foundation (2021JJ31116), Hunan Province Science and Technology Project (2021SK2021), and Guangxi Natural Science Foundation (2020GXNSFBA297082).

Funding This study was supported by National Natural Science Foundation of China, (Grant Nos. 81660273, 81672889, 82101907, 82060042, 32000665), Natural Science Foundation of Changsha, (Grant Nos. kq2014297, kq2202125), Natural Science Foundation of Hunan Province, (Grant No. 2021JJ31116), Hunan Provincial Science and Technology Department, (Grand No. 2021SK2021), Natural Science Foundation of Guangxi Province, (Grant No. 2020GXNSFBA297082).

Declarations

Conflict of interest The authors declare no conflict of interest.

References

Bellet M, Deriu E, Liu J et al (2013) Circadian clock regulates the host response to Salmonella. Proc Natl Acad Sci USA 110:9897–9902. https://doi.org/10.1073/pnas

Brandenburg K, Jürgens G, Müller M et al (2001) Biophysical characterization of lipopolysaccharide and lipid A inactivation by lactoferrin. Biol Chem 382:1215–1225. https://doi.org/10.1515/bc.2001.152

Campione E, Cosio T, Rosa L et al (2020) Lactoferrin as protective natural barrier of respiratory and intestinal mucosa against coronavirus infection and inflammation. Int J Mol Sci 21:4903. https://doi.org/10.3390/ijms21144903

Cutone A, Lepanto M, Rosa L et al (2019) Aerosolized bovine lactoferrin counteracts infection, inflammation and iron dysbalance in a cystic fibrosis mouse model of pseudomonas aeruginosa chronic lung infection. Int J Mol Sci 20:2128–2142. https://doi.org/10.3390/ijms20092128

Dal-Secco D, Wang J, Zeng Z et al (2015) A dynamic spectrum of monocytes arising from the in situ reprogramming of CCR2+ monocytes at a site of sterile injury. J Exp Med 212:447–456. https://doi.org/10.1084/jem.20141539

Domscheit H, Hegeman M, Carvalho N et al (2020) Molecular dynamics of lipopolysaccharide-induced lung injury in rodents. Front Physiol 11:36. https://doi.org/10.3389/fphys.2020.00036

Elzoghby A, Abdelmoneem M, Hassanin I et al (2020) Lactoferrin, a multi-functional glycoprotein: active therapeutic, drug nanocarrier & targeting ligand. Biomaterials 263:120355. https://doi.org/10.1016/j.biomaterials.2020.120355

Handley S, Dube P, Miller V (2006) Histamine signaling through the H(2) receptor in the Peyer's patch is important for controlling *Yersinia enterocolitica* infection. Proc Natl Acad Sci U S A 103:9268–9273. https://doi.org/10.1073/pnas.0510414103

Joo S, Park M, Kim K et al (2016) Cold stress aggravates inflammatory responses in an LPS-induced mouse model of acute lung injury. Int J Biometeorol 60:1217–1225. https://doi.org/10.1007/s00484-015-1116-5

Khaenam P, Rinchai D, Altman M et al (2014) A transcriptomic reporter assay employing neutrophils to measure immunogenic activity of septic patients' plasma. J Transl Med 12:65. https://doi.org/10.1186/1479-5876-12-65

Ley K, Laudanna C, Cybulsky M et al (2007) Getting to the site of inflammation: the leukocyte adhesion cascade updated. Nat Rev Immunol 7:678–689. https://doi.org/10.1038/nri2156

Liu Y, Perego M, Xiao Q et al (2019) Lactoferrin-induced myeloid-derived suppressor cell therapy attenuates pathologic inflammatory conditions in newborn mice. J Clin Invest 129:4261–4275. https://doi.org/10.1172/JCI128164

Luster A (1998) Chemokines–chemotactic cytokines that mediate inflammation. N Engl J Med 338:436–445. https://doi.org/10.1056/NEJM199802123380706

Lutaty A, Soboh S, Schif-Zuck S et al (2020) Resolution-associated lactoferrin peptides limit lps signaling and cytokine secretion from human macrophages. Int J Mol Sci. https://doi.org/10.3390/ijms21145166

Na Y, Stakenborg M, Seok S et al (2019) Macrophages in intestinal inflammation and resolution: a potential therapeutic target in IBD. Nat Rev Gastroenterol Hepatol 16:531–543. https://doi.org/10.1038/s41575-019-0172-4

Pammi M, Suresh G (2017) Enteral lactoferrin supplementation for prevention of sepsis and necrotizing enterocolitis in preterm infants. Cochrane Database Syst Rev 6:Cd007137. https://doi.org/10.1002/14651858.CD007137.pub5

Rittirsch D, Hoesel L, Ward P (2007) The disconnect between animal models of sepsis and human sepsis. J Leukoc Biol 81:137–143. https://doi.org/10.1189/jlb.0806542

Superti F (2020) Lactoferrin from bovine milk: a protective companion for life. Nutrients. https://doi.org/10.3390/nu12092562

Vannella K, Wynn T (2017) Mechanisms of organ injury and repair by macrophages. Annu Rev Physiol 79:593–617. https://doi.org/10.1146/annurev-physiol-022516-034356

Varela M, Mogildea M, Moreno I et al (2018) Acute inflammation and metabolism. Inflammation 41:1115–1127. https://doi.org/10.1007/s10753-018-0739-1

Velusamy S, Ganeshnarayan K, Markowitz K et al (2013) Lactoferrin knockout mice demonstrates greater susceptibility to *Aggregatibacter actinomycetemcomitans*-induced periodontal disease. J Periodontol 84:1690–1701. https://doi.org/10.1902/jop.2013.120587

Wang J, Kubes P (2016) A reservoir of mature cavity macrophages that can rapidly invade visceral organs to affect tissue repair. Cell 165:668–678. https://doi.org/10.1016/j.cell.2016.03.009

Wang B, Timilsena Y, Blanch E et al (2019) Lactoferrin: structure, function, denaturation and digestion. Crit Rev Food Sci Nutr 59:580–596. https://doi.org/10.1080/10408398.2017.1381583

Wei L, Zhang X, Wang J et al (2020) Lactoferrin deficiency induces a pro-metastatic tumor microenvironment through recruiting myeloid-derived suppressor cells in mice. Oncogene 39:122–135. https://doi.org/10.1038/s41388-019-0970-8

Wei L, Liu C, Wang J et al (2021) Lactoferrin is required for early B cell development in C57BL/6 mice. J Hematol Oncol 14:58. https://doi.org/10.1186/s13045-021-01074-6

Wu J, Hu Y, Du C et al (2016) The effect of recombinant human lactoferrin from the milk of transgenic cows on *Salmonella enterica* serovar typhimurium infection in mice. Food Funct 7:308–314. https://doi.org/10.1039/C5FO00817D

Xiao S, Zhou Y, Jia H et al (2021) Identification of the pivotal differentially expressed genes and pathways involved in *Staphylococcus aureus*-induced infective endocarditis by using bioinformatics analysis. Eur Rev Med Pharmacol Sci 25:487–497. https://doi.org/10.26355/eurrev_202101_24420

Xu J (2005) Preparation, culture, and immortalization of mouse embryonic fibroblasts. Curr Protoc Mol Biol. https://doi.org/10.1002/0471142727.mb2801s70

Ye Q, Zheng Y, Fan S et al (2014) Lactoferrin deficiency promotes colitis-associated colorectal dysplasia in mice. PLoS ONE 9:e103298. https://doi.org/10.1371/journal.pone.0103298

Zimecki M, Actor K, Kruzel L (2021) The potential for Lactoferrin to reduce SARS-CoV-2 induced cytokine storm. Int Immunopharmacol 95:107571. https://doi.org/10.1016/j.intimp.2021.107571